Influence of the spatial variation of upstream velocity on a vertical-axis tidal turbine performance

Lilia Flores Mateos, Carwyn Frost, Nicholas Baker-Horne, Louise Kregting, Vincent McCormack

Abstract—**A good assessment of the upstream flow field is key to evaluating the performance of a tidal energy converter (TEC). Devices with vertical axis turbines present multiple advantages; however, their operation near the sea surface causes difficulty in measuring the upstream flow due to the hydrodynamic conditions that prevail in coastal environments. A full-size version of Gkinetic CEFA 12 was tested in Strangford's Narrows, where high velocity tidal-driven currents are present. The floating device uses a bluff body to enhance the incoming flow to the two vertical axis rotors located at its port and starboard sides. Therefore, in addition to operating in the complex hydrodynamic conditions of the sea surface, the flow enhancer may alter the upstream flow, leading to an incorrect estimation of the tidal-stream resource as well as the device's performance. An experimental set-up is proposed to measure the upstream flow using acoustic Doppler profilers mounted on the TEC, following the recommendations of the IEC TS62600-200.**

The potential flow diversion produced by the rotor's operation was investigated using data sets of high current speeds obtained from the starboard and port sides of the TEC during conditions of operation and non-operation. The analysis within the top 4 m of the water column indicated that the velocity components V_y and V_z showed different i) vertical structures and ii) velocity intensification for increasing current speeds at the port and starboard sides. However, these differences have a minor effect because the resultant horizontal velocity obtained from V_x and V_y components tends to show a flow where the main direction is towards the rotors; meanwhile, V_z tends to show an upward flow.

The analysis indicates that when the device is operating, the extension of the bluff body does not alter the incoming flow at the sample point used (two equivalent diameters). Therefore, the experimental set-up presented is suitable to measure the undisturbed upstream flow of floating vertical axis TEC in coastal waters.

Index Terms—**Tidal-stream resource assessment, Undisturbed flow conditions, Full-size TEC operation, Currents vertical structure, Strangford Lough, Environmental monitoring, M_2 tidal ellipse parameters, Field campaign.**

This work was supported by CASE through Invest Northern Ireland (INI) grant RD0418916.

L. Flores Mateos is at Queen's University Belfast (e-mail: l.flores@qub.ac.uk)

C. Frost, N. Barker-Horne are at Queen's University Belfast.

L. Kregting was at Queen's University Belfast, she is now at the New Zealand Institute for Plant and Food Research Limited

V. McCormack is at Gkinetic Energy Ltd, Limerick, Ireland

Digital Object Identifier:
https://doi.org/10.36688/ewtec-2023-323

I. Introduction

The combination of both i) astronomical forcings that predictably drive tides on a large scale and ii) the characterisation of the local tidal-stream resource enables the determination and prediction of a site's energetic output with high confidence. This information is relevant not only to determining potential harvesting locations but also to identifying key places for TEC performance testing. At the local scale, tidal currents are enhanced by the seabed's topography and roughness. This is the case at the Queen's University Belfast (QUB) tidal test site located in the Narrows of Strangford Lough, which features a tidal channel ideal for testing TEC technology.

Operating a TEC in a coastal environment provides the developer with realistic test conditions to evaluate the performance of the device. Tidal test sites such as in Strangford Lough present unsteady flow conditions produced by locally generated turbulence and velocity variability [1]. Rough flow conditions are intensified at spring tides, and turbulence increases and varies over the water column [2]. These unsteady conditions have the capacity to reduce a TECs performance. However, realistic flows present an opportunity to test full size devices, obtain feedback on the design (structural strength, flotation, and anchoring), and gain operational experience at an affordable cost compared to laboratory testing [3].

Novel designs of vertical axis energy converters have been developed in recent years, such as the Gkinetic floating device that uses a bluff body to enhance the flow passing through the two rotors and extracts energy from near-surface currents [4]. The concept of GK has been tested at the $1:40$ scale in the NUI Galway tidal basin and at the $1:20$ scale in the IFREMER wave-current recirculating flume in Boulogne-Sur-Mer, France [5]. The testing of the bluff body without turbines reported an increase in the incoming free-stream speed by a factor of 2 [5]. On the other hand, a full size version of Gkinetic was tested in Strangford Lough, and results derived from it are reported in this manuscript. The capability of accelerating the incoming flow expands the areas of potential energy harvesting to less energetic sites such as shallow estuary environments, rivers, and man-made canals.

Also, vertical axis turbines are an attractive design because they respond to flow from any direction [6] such as the GKinetic device that operates on a single

point mooring, enabling passive flow alignment. The continuous repositioning of the device according to the prevailing tidal regime avoids difficulties with turbine orientation. Rotor alignment with the incoming flow adds complexity to conventional designs because energetic regions ideal for tidal-stream harvesting present some degree of flow direction and magnitude asymmetry between flood and ebb tides [7].

In terms of power production, some designs of vertical axis turbines that have been developed are in the order of kW in capacity in comparison to major tidal current turbines, which are in the order of MW [8]. However, this reduced power production is compensated by the i) wide spectrum of sites of application, ii) scalability of the device, and iii) modularity of its components [9]. Additionally, because vertical axis turbines are being designed to operate as floating devices, the processes of installation, maintenance, and retrieval are less demanding and only require a seabed mooring [1], [8]. A further benefit of a floating TEC is the reduced impact on the local hydrodynamics in terms of turbidity, salinity, and sediment movements [10]. The balance of these conditions is relevant in shelf environments such as estuaries, which are ecosystem niches [11], [12].

Vertical axis turbines developed for river and tidal applications are designed to operate floating [9], harvesting the kinetic energy available on the superficial currents. However, the devices proximity to the sea surface and the unsteady tidal conditions where they operate cause difficulties when measuring the upstream flow. Nevertheless, tracking the flow available is relevant to assessing the TECs performance. In the case of Gkinetic, the device uses a bluff body to divert the flow towards the rotors, and its extension may affect the upstream flow, leading to wrong estimations of the tidal-stream resource and device performance.

Consequently, the expansion of tidal-stream harvesting sites to include i) locations with less energetic tidal currents and ii) devices that harvest the kinetic energy available in the top third of the current flow leads to new research questions such as:

- How to assess the upstream flow of a full-size floating TEC under realistic flow conditions?
- How to maintain undisturbed conditions in the upstream flow assessment during TEC operation?

Within the framework of the Vertical Axis Tidal Turbines in Strangford Lough project (VATTS) campaigns to assess the tidal-stream resource, evaluate Gkinetic performance, and perform environmental monitoring have been carried out at the QUB's test site in Strangford Lough, Northern Ireland, UK.

The project aims to contribute to the development of carbon-neutral energy suppliers using river and tidal currents. An experimental set-up has been developed and tested to track the upstream flow of the Gkinetic device. To investigate whether the upstream flow is being contaminated during the device's operation, measurements from two acoustic Doppler profilers (ADP) mounted on the TEC were analysed. The recommendations of IEC-200 were followed when mounting the ADPs relative to Gkinetic's rotors. The measurements would indicate any tendency of the flow to divert as a result of the bluff body's presence and/or device operation.

Fig. 1. QUB test site at the Narrows of Strangford Lough, Northern Ireland. The yellow marker indicates the location of the bed-mounted ADCP and Gkinetic device deployment.

II. Methods

A. Study site

The study site is at QUB's test site in Strangford Lough, on the East side of Northern Ireland (Figure 1). Evaluation of the tidal-stream resource was performed at $54°22.87$ N and $05°33.38$ W location, where an Acoustic Doppler Current Profiler (ADCP) was bed-mounted and the Gkinetic device was deployed. This place is situated in the narrow channel that connects the main body of the Lough to the Irish Sea [13]. The channel is known as the Strangford's Narrows and is a highly energetic area [3]. The channel is 8 km in length and has a minimum width of 0.5 km; it is characterized by its wave-sheltered environment [14]. Higher flows are observed in the channel at depths ($25< H <60$ m), and slower flow conditions are observed towards the sides where it is shallower. The site investigated presents a mean depth of $\sim$18 m. The currents in the Lough are mainly driven by astronomic tides with a semidiurnal frequency [15].

B. Experimental set-up

The full scale 12KW Gkinetic (GK) device consists of two 1.2 m vertical axis turbines attached to the sides of a buoyant platform, which uses a bluff body to accelerate the incoming flow to the rotors (Figure 2). The performance of the device was consistent during operating conditions (control system and pitch system).

The tidal-stream resource was assessed at approximately the same location of TEC operation considering two scenarios: 1) currents at undisturbed conditions i.e. no presence of the device, and 2) currents during the deployment.

The first scenario was studied using data from an RDI sentinel V50 ADCP with 5 beams, which was mounted on the seabed prior to the device's deployment (data-set 1 in Table I). The bed-mounted ADCP current measurements were taken with sampling intervals of 1 s and 10 s using 0.50 m cell-size, but the

time series analysed were reduced to 60 s sampling rate. A data quality control was performed to remove anomalous velocity data near the surface produced by side-lobe interference. The final profile accounting for the blanking distance consisted of 24 vertical cells extending from ∼0.65 m above the seabed up to 13.8 m.

For the second scenario, the upstream flow was measured using two Nortek 2 MHz Aquadopp profilers with 3 beams (AQP). On the port and starboard (Stb) sides of the device, an AQP was mounted using a truss assembled to the platform of the device. A distance of two equivalent diameters ($2D_E$) was left from the AQP's to the rotors following recommendations of IEC-200 [16], where $2D_E$ =3.92 m.

The equivalent diameter is a function of the device's projected capture area (A). In the case of GK, the projected capture area of each rotor was estimated by considering half of the bluff body. Therefore, per each rotor, the corresponding area is $A = A_r + \frac{1}{2}A_b$, where A_r and A_b stand for rotor area and bluff-body area, respectively. The bluff body was included in the D_E calculation because the structure acts as a hydrodynamic component that enhances the flow thereof, favouring energy conversion [17]. As [5] indicates, the presence of the bluff body increases the capture area of the device and avoids the need for larger and more expensive turbines.

The use of two AQP with the same technical specifications avoids disparity in the measurements, which can occur when combining different sensors [2]. The AQP's were aligned to the rotors, and to reduce any disturbance from the platform, a distance of ∼ 1.21 m was kept at a depth of 0.40 m. The Port-AQP and Stb-AQP mounted on the device collected current velocities with sampling intervals of 60 s and 20 s respectively, using 0.20 m cell-size. The different sampling rate is due to the memory capacity of each sensor. The quality control consisted of the removal of unreliable velocity data due to low and/or peak echo intensity amplitudes. A signal to noise ratio was estimated as a function of the amplitude, and data-points with a signal to noise ratio larger than 70 and lower than 15 were discarded. The final profile accounting for the blanking distance consisted of 20 vertical cells starting from a near-surface depth. On average, the profile extended from ∼0.5 m to ∼4 m below the sea surface. While three campaigns were performed for the second scenario (device-mounted instruments), as the aim of this manuscript was to determine if the upstream flow is being contaminated during the device operation, only the first deployment is being reported (data-set 2 in Table I).

The ADCP and AQPs were calibrated according to the manufacturer's recommendations. For the analysis, raw velocity measurements collected with the ADCP were converted to the Earth coordinate system (ENU) as the ADCP held a geostationary position. In the case of AQP's data, the use of the Cartesian coordinate system (XYZ) facilitated the analysis (Figure 2). Because of the passive flow alignment of the device, the AQP's main heading direction is $x-$component at flood and ebb tides.

TABLE I
CURRENTS DATA-SETS COLLECTED DURING VATTS

Dataset	Scenarios description	Orientation	Dataset description	Instrument	Sampling rate	Data recorded
1	Data from sea-bed mounted instrument	Fix and upward facing	Undisturbed conditions campaign	ADCP sentinel V	dt=60 sec	01 Oct-17 Nov 2021
2	Data from device mounted instrument	Passive flow alignment and downward facing	First device deployment. **Low-flow site**	AQP – Port	dt=60 sec	18-25, Jan 2022
				AQP – Starboard	dt=20 sec	
3				AQP – Port	dt=60 sec	25 Jan-14 Feb 2022
4			Second device deployment. **Low-flow site**	AQP – Port	dt=1 sec	06-09, Jun 2022
				AQP – Starboard		
5			Third device deployment. **High-flow site**	AQP – Port	dt=1 sec	10-13, Jun 2022
				AQP – Starboard		

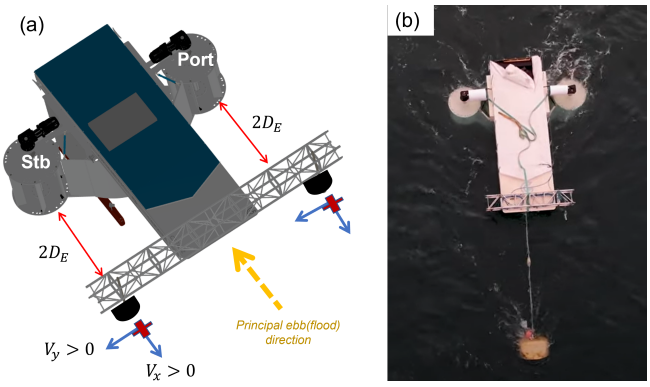

Fig. 2. Plan-view of the experimental set-up sketch (a), at the port and starboard (Stb) sides of the device an AQP was located, leaving two equivalent diameters ($2D_E$) from the rotors. The two AQP's were facing downward and in the direction opposite the rotors. Consequently, the incoming flow is shown as negative. TEC in operation at the site (b).

In terms of tidal conditions during the deployment, the forecast of the sea level obtained from tidal harmonic analysis (HA) of data-set 1 (HA further description is described in subsection III-A) indicates spring tides during the measurements collection of data-set 2 (18-25 Jan, 22). Despite the fact that the tides were not as strong as in early Jan 2022, the currents still represent good conditions for device operation. Regarding current speed, the forecast of the tidal currents at 13.8 m from the seabed indicates peak velocities of 2.5 m/s during the period of observation.

In terms of operating conditions, the device was deployed on the site at a single point mooring, enabling passive flow alignment. The device operated during daylight hours at high flood and ebb current speeds. The time of operation varied from 3.5 to 6.5 hrs. To investigate if device operation has an influence on the incoming flow, two situations were investigated: Operating Condition (OC) and Non-Operating Condition (Non-OC). Three days of turbine operation were identified: 19, 20, and 21 of January 2022, during these days the AQP at the Stb and port sides were collecting data simultaneously (Figure 3). For the comparison, the Non-OC events selected presented similar current conditions and duration to the OC events.

During the device operation, environmental moni-

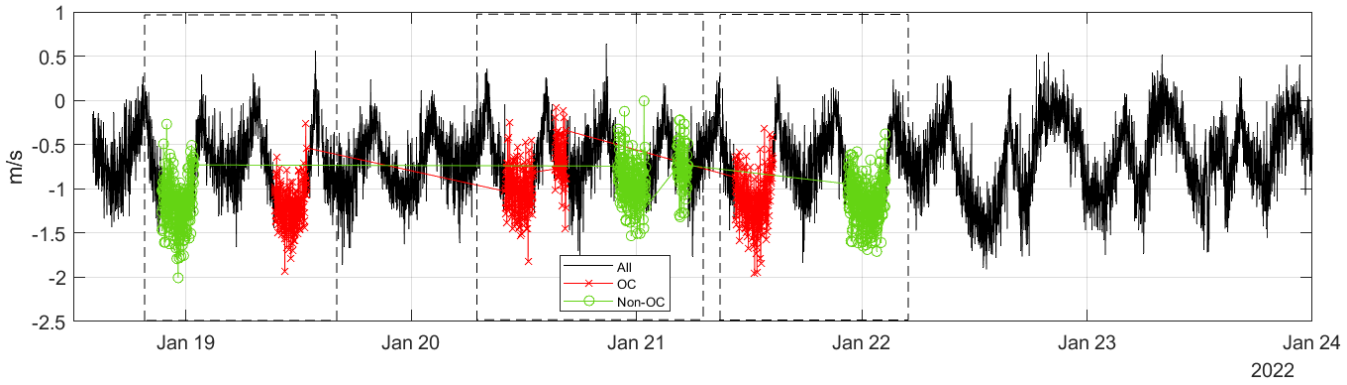

Fig. 3. Data-set 1, V_x component time-series from AQP port side shallower bin. The three events investigated are shown in black dash-line rectangles. The events include OC and Non-OC situations, a similar dataset was obtained for Stb side.

Fig. 4. The port side cameras with the rotor facing (right) and forward-facing (left) cameras showed. This is after the device was removed showing no signs of fouling on the cameras.

toring of the device was undertaken. Firstly, the marine mammal observers (MMOs) were observing for the presence of marine mammals within 50 m of the device. This was required under the Marine Licence (ML20_21011) with a shutdown protocol, meaning that the device was required to be stopped if a marine mammal was sighted within 50 m of the device. Further to MMOs, underwater cameras (Figure 4) were installed for monitoring of the turbines below the water [18]. Video was recorded and analysed after collection for collisions and the passage of animals near the device. There were 17 marine mammal sightings and 7 shutdowns over the total operational period (18 Jan - 13 Jun, 22). No collisions or indications of harm were witnessed during the operation of the device or in the analysed video footage.

III. Results

A. Undisturbed conditions

To identify the current vertical profile under undisturbed conditions of the flow at the test side, a tidal harmonic analysis was performed on the 46 days collected by the seabed mounted ADCP. T_tide Matlab package [19] was used for the analysis, which indicated that tidal forcing explains more than 94% variance of the currents within 77% of the water column (13.8 m from the seabed). For depths shallower than 13.8 m the variance explained, and the signal-to-noise ratio (SNR) decreased as data is lost due to side lobe interference. The SNR is a ratio defined in terms of the tidal current ellipses' parameters as $SNR = (M_{axis}/E_M)$, where M_{axis} refers to the constituent major axis and E_M to the error at a 95% confidence interval for the major axis. The SNR is an indicator of the strength of the tidal constituent, with 35 constituents resolved for the Narrows (Figure 5). The main frequencies that influence the temporal variability at the site are: the principal lunar (M_2), principal solar (S_2), larger lunar elliptic (N_2), luni-solar declinational (K_1), larger lunal declination (O_1) and the overtide M_4, whose period of 6.21 hr is a multiple of M_2 [20].

Within 77% of the water column, the M_2 ellipse parameters indicate that the maximum current velocity (major axis) tends to increase towards shallower depths, meanwhile the minimum current velocity (minor axis) shows a slight decrease. The minor axis small values describe a strong unidirectional current over the water column, which is orientated $\sim 128°$ for ebb tide and $\sim 308°$ for flood tide. The uniform phase indicates that the maximum current occurs simultaneously over the water column.

B. Device presence and operation

Measurements from the AQP's at the port and Stb side were used to investigate any tendency that the flow was diverted due to the bluff body's presence and device operation. The analysis that follows was performed on the OC and Non-OC events identified on the 19, 20, and 21 of January 2022 (Figure 3). As similar results were obtained from all three days, only 21 Jan, 22 is shown as an example in this manuscript. The duration of the OC and Non-OC events on this day was 4 hrs.

To identify any effect of the device operation throughout the top 4 m of the water column, the vertical profiles of the currents with speeds higher than 1 m/s were compared during OC and Non-OC conditions (Figure 6). This velocity threshold was

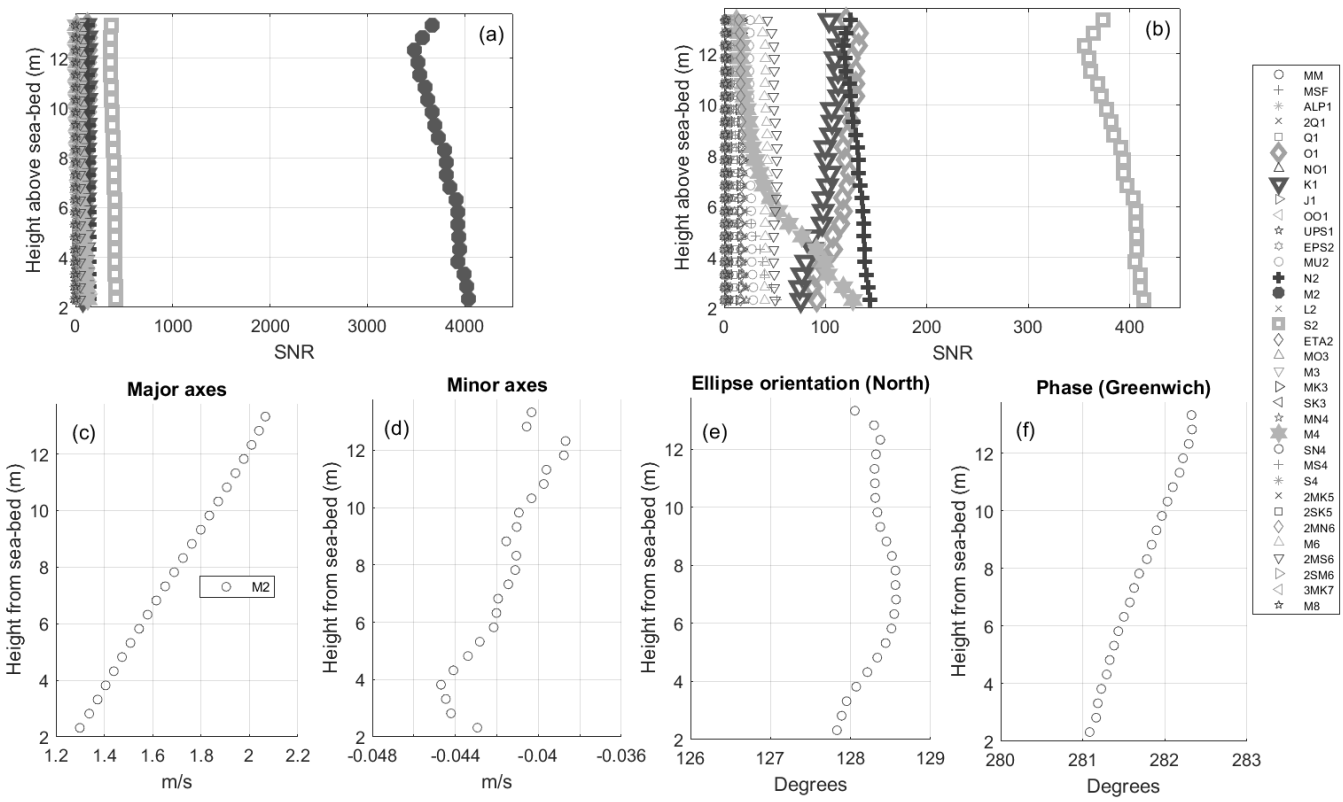

Fig. 5. Signal noise ratio of tidal constituents over 77% of the water column (a), zoom-in (b). M_2 ellipse parameters during undisturbed conditions: major axes (c), minor axes (d), orientation (e), and phase (f).

selected to focus on currents relevant to the device's operation.

For depths deeper than 2.5 m the current speed (CS) and V_x vertical profiles experienced an intensification due to the higher current speed observed with the HA at the M_2 major axis (Figure 6 a and b). Also, it is observed a reduction in the magnitudes fluctuation within this depth during OC conditions. This magnitude reduction is also reflected in the smaller vertical gradient observed in CS and V_x during OC (Figure 6 e and f).

Within the top 4 m the velocity components V_y and V_z profiles (Figure 6 c and d) differ according to the AQP's side; however, this influence is more evident on V_z. Also, for depths greater than 2.5 m the OC tends to reduce both the magnitude of the components and the vertical velocity gradient (Figure 6 g and h).

Figure 7 shows the profiles within the top 2 m, V_x is the main contributor to the current speed, and neither the CS nor V_x profiles show a substantial difference between the port and Stb side (Figure 7 a and b). Operating conditions seem to induce a slight magnitude increase on both sides however, the increase is negligible. The similarity between the CS and V_x profiles independently of the AQP's location and operating conditions may suggest that the upstream flow can be measured from a single side.

Velocity components V_y and V_z are more sensible to the side location, and profiles tend to be consistent over depth (Figure 7 c and d). In the case of V_y stb-side profiles are stronger and suggest a flow direction tendency towards the rotor (see $V_y < 0$ in Figure 2). On the port side V_y shows a slight decrease in magnitude; this reduction may indicate a tendency for the flow to change direction towards the rotor. Similarly, V_z at the Stb side has a stronger profile ($V_z < 0$) that indicates an upward direction of the flow; at the port side, V_z weakens and may lead to a downward flow direction. OC seems to slightly affect the profiles of V_y and V_z however, the location of the instruments has a stronger impact on the profiles.

To identify if the upstream flow direction is influenced by the device at higher speeds, the V_x velocity was separated into bin velocity increments of 0.1 m/s, from 1 m/s to 2.5 m/s. Once V_x velocities were allocated in bins, V_x indices were used to identify the corresponding values of V_y and V_z.

The analysis of shallow depths within 0.6 - 1.4 m shows a similar behaviour, which is exemplified by the depth at 0.6 m from the sea surface. For 1< V_x <1.4 m/s, V_x increment produced relative consistent values of V_y (Figure 8a). Stb side tends to present stronger magnitudes of V_y ($V_y < 0$), and port side tends to present smaller magnitudes. During OC, V_y at the port side tends to reduce and become $V_y > 0$ occasionally (considering the three events analysed). For $V_x > 1.4$ m/s, V_y magnitude changes; however, based on the analysis of the three events, the tendency is not clear (Figure 8b). Also, it is not possible to relate V_y changes to AQP's side or conditions of operation. Similarly, V_z presented consistent values for 1< V_x <1.4 m/s. At Stb side V_z tends to present stronger magnitudes than port side, during OC V_z port side shows magnitudes comparable to Stb side. For $V_x > 1.4$ m/s, the tendency

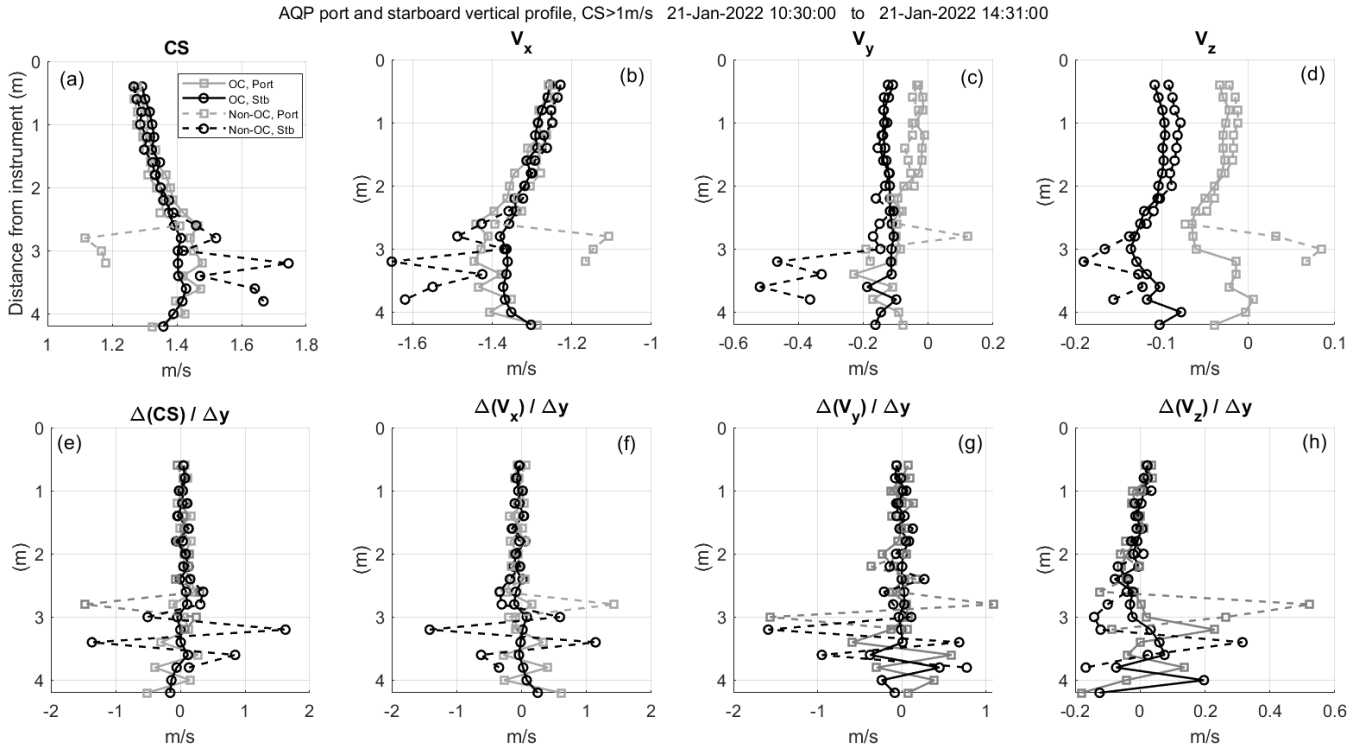

Fig. 6. Vertical profile over the top 4 m obtained from the temporal average of current speeds $> 1\ m/s$. Current speed (a), V_x (b), V_y (c), and V_z (d) velocity components. Vertical speed gradient of the current speed (e), V_x (f), V_y (g), and V_z (h)

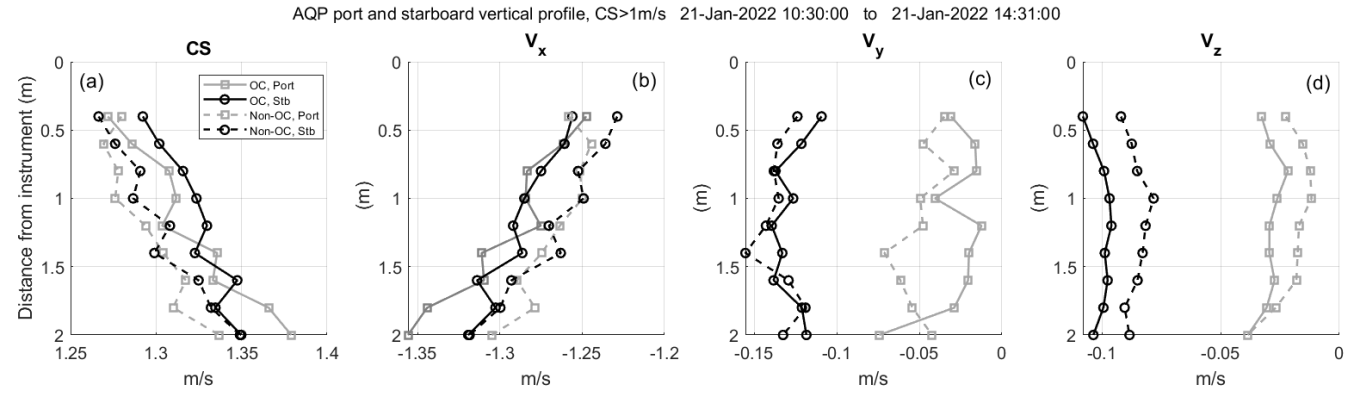

Fig. 7. Vertical profile over the top 2 m obtained from the temporal average of current speeds $> 1\ m/s$. Current speed (a), V_x (b), V_y (c), and V_z (d) velocity components.

of V_z is not clear.

For depths deeper than 1.4 m, values of V_y and V_z seem to fluctuate independently of V_x increases (Figure 8 c and d). Additionally, there is no clear influence of the AQP's side and operation conditions, and this is more evident on V_z which show similar values for the four situations.

IV. Discussion and Conclusion

A reliable assessment of the upstream flow available to the TEC is key to evaluating its performance. The Gkinetic device uses a bluff body to accelerate the incoming flow to the rotors, thereby enhancing the flow by a factor of 2 [5]. However, there is a risk that the bluff body volume may influence the incoming flow measured by the AQP's, therefore contaminating the upstream flow and providing misleading estimations of the tidal resource.

Additionally, the measurement of the upstream flow during operation becomes challenging due to the proximity of the device to the sea surface. Assessment of the shallow-depth currents is not feasible with a seabed mounted ADCP as side-lobe interference produces loss of data points at the depths where the floating device operates. A turnaround to this issue is the superficial platform of Gkinetic, which enabled the mounting of two AQPs at a distance of 2 D_E from the rotors.

Three days (19, 20, and 21 of January 2022) were used to investigate whether the device's flow enhancer and/or its operation had an impact on the upstream flow. During these dates, data from the AQPs located at the Stb and port sides of the device were analysed during OC and Non-OC conditions.

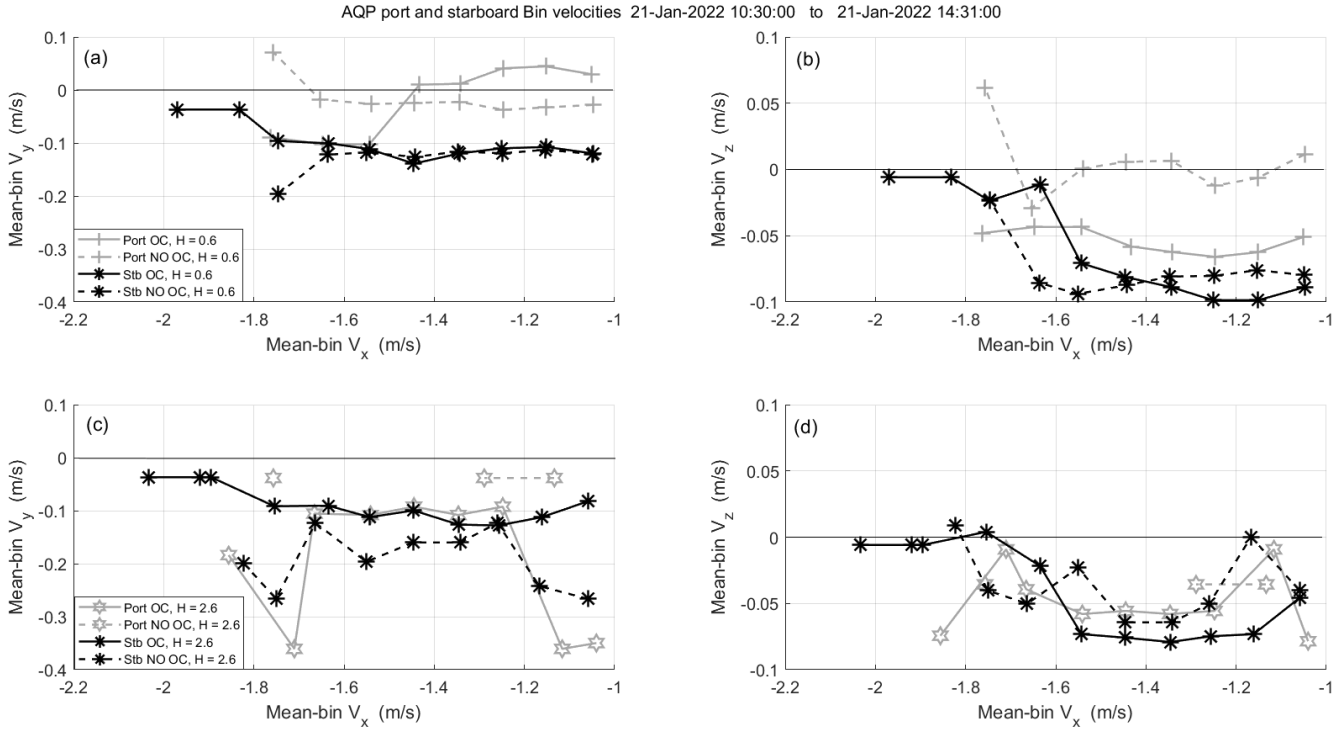

Fig. 8. V_x velocity bins and corresponding V_y (a) and V_z values (b) at a shallow depth (6 m from the sea surface). V_x velocity bins and corresponding V_y (c) and V_z values (d) at a deeper depth (2.6 m from the sea surface).

The velocities vertical profile for speeds relevant to the device operation ($CS > 1\ m/s$) indicates that the current speed and V_x profiles are similar within the top 2 m, independently of the AQP's location and operating conditions. At depths deeper than 2.5 m, the magnitudes increase and the vertical velocity gradient indicates that the increase occurs at a higher rate, especially during Non-OC; similar behaviour was observed in V_y and V_z velocity components. The current speed intensification at depths $>$ 2.5 m from the sea surface is explained by the presence of high current speeds observed with the M_2 tidal ellipse parameters. The M_2 constituent is the most relevant constituent at the site, and the major axis shows that the highest current speed takes place at 13.8 m from the seabed (Figure 6), this depth corresponds to 77% of the water column. Intensification of the velocity profile within the 77% of the water column is consistent with the velocity profile presented at potential tidal-stream sites [21]; variations of the velocity profile are related to stratification and small scale bathymetric variations [22].

The influence of the AQP's location is more evident on the V_y and V_z components, within the top 2 m V_y at the Stb side, which presented higher and negative magnitudes describing flow towards the rotor (Figure 9); meanwhile, the port side presents smaller magnitudes. On the other hand, the bin analysis shows that as V_x increases,the values of V_y and V_z at the Stb side in the shallow depths (top 1.4 m) are stronger within the range $1< V_x <1.4\ m/s$ independently of the operating conditions. In the case of the port side, the device operation has a stronger effect; during this condition, V_y weakens and becomes occasionally positive, suggesting a weak flow direction towards the rotor (Figure 9). In terms of V_z, it increases and becomes negative during OC, indicating an upward flow direction. The stronger flow observed on the Stb side of the device, could be driven by local bathymetric features.

Evaluation of OC and Non-OC conditions suggests that the device operation does not generate a flow diversion within the velocity range $1< V_x < 1.4\ m/s$ at shallow depths ($0.6 < H < 1.4\ m$), and the measurements indicate that the flow tends to head towards the rotors. For $V_x > 1.4\ m/s$ the values of V_y change without a clear relation to the conditions of operation or as a result of the AQP's side location; however, V_y does not suggest flow diversion.

Consideration of the Stb and port sides shows an influence on V_y and V_z however, the following findings indicate that this effect is minor:

- Lack of flow diversion on V_y for increasing values of V_x.
- Lack of significant velocity gradient over the top 2 m on V_x, V_y, and V_z suggests a consistent rate of velocity change over the vertical. A small effect on the current's velocity gradient throughout the water column is expected from devices with a relative small rotor diameter [13].
- Lack of V_x reduction during turbine operation. Velocity reduction during turbine operation is associated with increasing the device's blockage ratio [23].
- V_x is almost one order of magnitude higher than V_y within the top 4 m.

Therefore, the extension of the bluff body and the device operation do not seem to have a significant effect on currents greater than 1 m/s. It is possible to assume that undisturbed conditions are being measured with

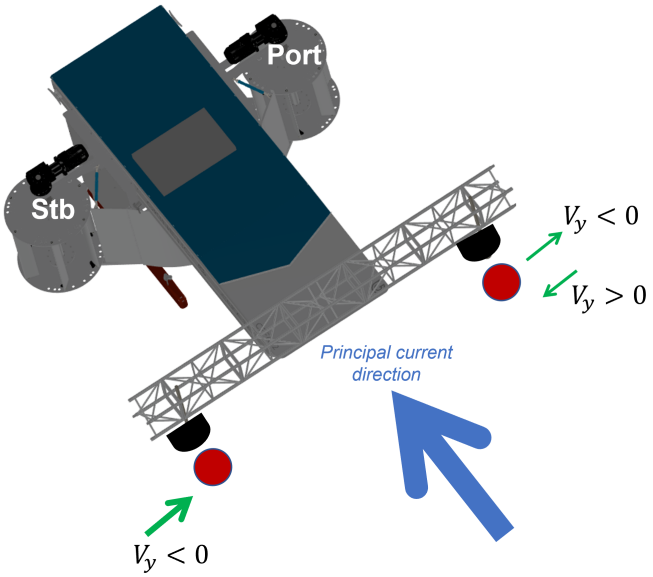

Fig. 9. Schematic resultant circulation during turbine operation, within $1< V_x < 1.4\ m/s$ and shallow depths ($0.6 < H < 1.4\ m$). Red circles indicate an upward flow direction.

the AQPs mounted on the device. The following steps are to identify if the presence of the device at Non-OC is influencing the incoming flow, and to use a larger data-set from a single side location to assess the variation of the upstream condition (dataset-3 in table I). In conclusion, in line with the global challenge of harvesting marine renewable energy, we have developed and tested an experimental set-up that enables the measurement of the upstream flow during the device's operation in coastal waters. The set-up complies with IEC-200 requirements and facilitates tracking the inflow during operation near the surface, providing confidence in the flow measurements obtained.

ACKNOWLEDGEMENT

This work is supported by the Centre for Advanced Sustainable Energy (CASE). CASE is funded through Invest NI's Competence Centre Programme and aims to transform the sustainable energy sector through business research.

REFERENCES

[1] C. Frost, I. Benson, P. Jeffcoate, B. Elsäßer, and T. Whittaker, "The effect of control strategy on tidal stream turbine performance in laboratory and field experiments," *Energies*, vol. 11, no. 6, 2018.

[2] C. Frost, M. Togneri, P. Jeffcoate, T. Lake, C. Boake, R. Starzmann, and A. Williams, "A comparison of platform and sea-bed mounted flow measurement instrumentation for SME PLAT-I," *International Marine Energy Journal*, vol. 5, no. 2, pp. 195–200, 2022.

[3] P. Schmitt, S. Fu, I. Benson, G. Lavery, S. Ordoñez-Sanchez, C. Frost, C. Johnstone, and L. Kregting, "A Comparison of Tidal Turbine Characteristics Obtained from Field and Laboratory Testing," *Journal of Marine Science and Engineering*, vol. 10, no. 9, 2022.

[4] B. A. Mannion, B. Eng, S. Nash, and S. Leen, "Combined Experimental Testing and Numerical Modelling of a Novel Vertical Axis Tidal Turbine," Ph.D. dissertation, NUIG, 2014.

[5] B. Mannion, V. McCormack, C. Kennedy, S. B. Leen, and S. Nash, "An experimental study of a flow-accelerating hydrokinetic device," *Proceedings of the Institution of Mechanical Engineers, Part A: Journal of Power and Energy*, vol. 233, no. 1, pp. 148–162, feb 2019.

[6] B. Yang and C. Lawn, "Fluid dynamic performance of a vertical axis turbine for tidal currents," *Renewable Energy*, vol. 36, no. 12, pp. 3355–3366, 2011.

[7] M. Thiébaut and A. Sentchev, "Asymmetry of tidal currents off the W.Brittany coast and assessment of tidal energy resource around the Ushant Island," *Renewable Energy*, vol. 105, pp. 735–747, 2017.

[8] R. Rosli and E. Dimla, "A review of tidal current energy resource assessment : Current status and trend," in *5th International Conference on Renewable Energy: Generation and Applications (ICREGA'18)*, no. February, 2018.

[9] M. J. Khan, G. Bhuyan, M. T. Iqbal, and J. E. Quaicoe, "Hydrokinetic energy conversion systems and assessment of horizontal and vertical axis turbines for river and tidal applications: A technology status review," *Applied Energy*, vol. 86, pp. 1823–1835, 2009.

[10] S. Barbarelli and B. Nastasi, "Tides and Tidal Currents—Guidelines for Site and Energy Resource Assessment," *Energies*, vol. 14, no. 6123, p. 20, 2021.

[11] P. A. J. Bonar, I. G. Bryden, and A. G. L. Borthwick, "Social and ecological impacts of marine energy development," *Renewable and Sustainable Energy Reviews*, vol. 47, pp. 486–495, 2015.

[12] S. P. Neill, K. A. Haas, and J. Thiébot, "A review of tidal energy — Resource, feedbacks, and environmental interactions," *Journal of Renewable and Sustainable Energy*, vol. 062702, no. November, 2021.

[13] P. Jeffcoate, R. Starzmann, B. Elsaesser, S. Scholl, and S. Bischoff, "Field measurements of a full scale tidal turbine," *International Journal of Marine Energy*, vol. 12, pp. 3–20, 2015. [Online]. Available: http://dx.doi.org/10.1016/j.ijome.2015.04.002

[14] A. Davison and T. Mallows, "Strangford Lough Marine Current Turbine," Royal Haskoning LTD Environment, Tech. Rep. January 2004, 2005.

[15] L. Kregting and B. Elsäßer, "A hydrodynamic modelling framework for strangford lough part 1: Tidal model," *Journal of Marine Science and Engineering*, vol. 2, no. 1, pp. 46–65, mar 2014.

[16] *IEC TS 62600-200 Marine energy - Wave, tidal and other water current converters – Part 200: Electricity producing tidal energy converters – Power performance assessment* , 2013.

[17] *IEC TS 62600-300 Marine energy - Wave, tidal and other water current converters - Part 300: Electricity producing river energy converters-Power performance assessment*, 2019.

[18] N. Baker-horne, L. Kregting, L. Flores Mateos, and C. Frost, "Environmental monitoring for VATTS project," Queen's University Belfast, Tech. Rep., 2023.

[19] R. Pawlowicz, B. Beardsley, and S. Lentz, "Classical tidal harmonic analysis including error estimates in MATLAB using TDE," *Computers and Geosciences*, vol. 28, no. 8, pp. 929–937, 2002.

[20] J. Gómez-Valdés, J. A. Delgado, and J. A. Dworak, "Overtides, compound tides, and tidal-residual current in Ensenada de la Paz lagoon, Baja California Sur, Mexico," *Geofísica Internacional*, vol. 42, no. 4, pp. 623–634, 2003.

[21] M. Lewis, S. P. Neill, P. Robins, M. R. Hashemi, and S. Ward, "Characteristics of the velocity profile at tidal-stream energy sites," *Renewable Energy*, vol. 114, pp. 258–272, 2017. [Online]. Available: http://dx.doi.org/10.1016/j.renene.2017.03.096

[22] L. Manuel, L. Flores-Mateos, and Candela-Pérez J., "Tidal currents at the sills of the Northern Gulf of California," *Continental Shelf Research*, vol. 227, pp. 1–14, 2021. [Online]. Available: https://www.sciencedirect.com/science/article/pii/S0278434321001692

[23] L. M. Flores Mateos and M. Hartnett, "Hydrodynamic Effects of Tidal-Stream Power Extraction for Varying Turbine Operating Conditions," *Energies*, vol. 13, no. 3240, p. 3240, 2020. [Online]. Available: http://dx.doi.org/10.3390/en13123240